REPORT DOCUMENTATION PAGE

1. AGENCY USE ONLY (Leave blank)	2. REPORT DATE	3. REPORT TYPE AND DATES COVERED
		FINAL REPORT 01 May 95 - 30 Apr 97

4. TITLE AND SUBTITLE

(AASERT-95) Precision Measurements with Hydrogen and Rubidium Masers

6. AUTHOR(S)

Dr Walsworth

5. FUNDING NUMBERS

61103D
3484/TS

AFOSR-TR-97

0351

7. PERFORMING ORGANIZATION NAME(S) AND ADDRESS(ES)

Smithsonian Astrophysical Observatory
60 Garden Street
Cambridge, MA 02138

9. SPONSORING/MONITORING AGENCY NAME(S) AND ADDRESS(ES)

AFOSR/NE
110 Duncan Avenue Suite B115
Bolling AFB DC 20332-8050

10. SPONSORING/MONITORING AGENCY REPORT NUMBER

F49620-95-1-0356

11. SUPPLEMENTARY NOTES

12a. DISTRIBUTION/AVAILABILITY STATEMENT

12b. DISTRIBUTION CODE

13. ABSTRACT (Maximum 200 words)

This AASERT grant supported Ph.D. thesis research on two new atomic clocks: the cryogenic hydrogen maser and the double-bulb rubidium maser. The cryogenic hydrogen maser (CHM) operates at low temperatures, and may provide frequency stability that is one to three orders of magnitude better than a room temperature hydrogen maser because of greatly reduced thermal noise and larger signal power. The double-bulb rubidium maser (DBRM) may have frequency stability comparable to that of a room temperature hydrogen maser but in a smaller, more robust, and lower cost package.

14. SUBJECT TERMS

15. NUMBER OF PAGES

16. PRICE CODE

17. SECURITY CLASSIFICATION OF REPORT	18. SECURITY CLASSIFICATION OF THIS PAGE	19. SECURITY CLASSIFICATION OF ABSTRACT	20. LIMITATION OF ABSTRACT
UNCLASSIFIED	UNCLASSIFIED	UNCLASSIFIED	UNCLASSIFIED

DTIC QUALITY INSPECTED 3

Precision measurements with hydrogen and rubidium masers

AFOSR Grant F49620-95-1-0356

Final Technical Report

For the period 1 May 1995 through 30 April 1997

PRINCIPAL INVESTIGATOR
Dr. Ronald L. Walsworth

August 1997

The Smithsonian Astrophysical Observatory
is a member of the
Harvard-Smithsonian Center for Astrophysics

19971006 000

DTIC QUALITY INSPECTED 3

OBJECTIVES

This AASERT grant supported PhD thesis research on two new atomic clocks: the cryogenic hydrogen maser and the double-bulb rubidium maser. The cryogenic hydrogen maser (CHM) operates at low temperatures, and may provide frequency stability that is one to three orders of magnitude better than a room temperature hydrogen maser because of greatly reduced thermal noise and larger signal power. The double-bulb rubidium maser (DBRM) may have frequency stability comparable to that of a room temperature hydrogen maser but in a smaller, more robust, and lower cost package.

BACKGROUND

At present, the room temperature atomic hydrogen maser is the most stable time and frequency source available for intervals from seconds to days. Hydrogen masers are *active oscillators* that operate at 1420 MHz on the $F = 1$, $m_F = 0 \rightarrow F = 0$, $m_F = 0$ hyperfine transition in the hydrogen electronic ground state. The frequency stability of state-of-the-art hydrogen masers, such as those designed and constructed by our group at the Smithsonian Astrophysical Observatory (SAO), is typically on the order of one part in 10^{15} for averaging intervals of 10^3–10^4 seconds. The hydrogen maser is an essential atomic clock for radio astronomy, time-keeping, and spacecraft navigation, and is used in precision tests of gravitation, relativity, and quantum mechanics [1]. For example, hydrogen masers developed at SAO are used in NASA's Deep Space Tracking Network, and in the U.S. Naval Observatory's ensemble of master clocks. A hydrogen maser built by our group at SAO was flown on NASA's Gravity Probe A [2], providing the most accurate test to date of the gravitational red-shift (a consequence of the local position invariance of the Einstein Equivalence Principle). Hydrogen masers are also valuable instruments for experimental atomic physics [3], including work at low temperatures [4].

The cryogenic hydrogen maser (CHM) operates at 0.5 kelvin, employing superfluid helium-coated walls to store the masing hydrogen atoms [5]. The CHM may provide frequency stability that is one to three orders of magnitude better than a room temperature hydrogen maser because of greatly reduced thermal noise and larger signal power. Such exceptional frequency stability will be required for spacecraft tracking in future deep-space missions, for space-based tests of relativity and gravitation, and for local (i.e. flywheel) oscillators used with "next-generation" absolute frequency standards such as the laser-cooled cesium fountain [6] and the linear ion trap [7]. These new devices, which are under development at NIST and other

laboratories, are *passive high-resolution frequency discriminators*. Alone, they cannot function as superior atomic clocks; their effective operation depends critically on being integrated with an *active* local oscillator with excellent short term stability--such as that expected from the CHM. The CHM will also be used to study important effects in low temperature atomic physics, including atomic hydrogen spin-exchange collisions and hydrogen–helium interactions.

The double bulb rubidium maser (DBRM) may provide short term frequency stability superior to that of a room temperature hydrogen maser, but in a unit that is smaller, lighter, more robust, and less expensive to manufacture. The advantageous properties of the DBRM, relative to the hydrogen maser, result from its higher operating frequency (6.835 GHz for the ^{87}Rb hyperfine transition) and simpler construction. Furthermore, the DBRM employs a novel two-chamber, coated-wall design to avoid the main performance limitations of traditional rubidium atomic clocks ("light shifts" and "pressure shifts"). Because it would provide excellent frequency stability in a compact and affordable package, the DBRM has wide potential usage in a variety of earth- and space-based atomic clock applications. For example, the DBRM could be a robust and inexpensive replacement for the hydrogen maser as the local oscillator for radio astronomy Very Long Baseline Interferometry (VLBI) and deep-space telemetry. The small size and weight, and high performance of the DBRM would also make it attractive for airborne and space-based applications. For example, the DBRM could be ideal as an improved clock for Global Positioning System (GPS) satellites, could increase the precision of locating geosynchronous spacecraft when used in conjunction with an on-board GPS receiver, and could improve the reliability of the Federal Aviation Administration's enhanced GPS system of aircraft navigation. In addition, the DBRM could be useful for airborne multistatic radar, for high-precision global time transfer, for space-based VLBI, and for space-based experiments in relativity and gravitation. Like the CHM, the DBRM could serve as the essential flywheel oscillator for next-generation absolute frequency standards.

CHM RESULTS

- We operated the CHM with a maximum hydrogen flux into the maser cavity $\approx 10^{12}$ atoms/sec, resulting in a maximum signal power $\approx 10^{-12}$ watts and a maximum stored hydrogen density $\approx 10^{10}$ cm^{-3}.

- We measured the CHM signal frequency as a function of temperature. The CHM's frequency is decreased by hydrogen collisions both with the

helium-film-coated walls of the storage chamber and with the helium vapor. These two hydrogen-helium collision processes each lower the CHM signal frequency but have opposite trends with temperature: the hydrogen-film interaction increases at lower temperature while the helium vapor pressure increases at higher temperature. Thus there is a minimum in the magnitude of the net hydrogen-helium frequency shift. For the current CHM geometry we measured this frequency shift minimum to occur near 0.53 K. At the hydrogen-helium frequency shift minimum the sensitivity of the CHM frequency to temperature variations will be minimized (a second-order dependence).

- We measured the CHM's line quality factor to be $\approx 2.3 \times 10^9$, implying that the atomic de-coherence (or T_2) time is 0.52 seconds. The contribution to T_2 from hydrogen escape from the resonant cavity is calculated from geometry to be approximately 2.5 seconds. The measured contributions to T_2 from magnetic field gradients and hydrogen-hydrogen collisions are also small. Thus the observed T_2 is primarily due to hydrogen relaxation on the helium-film covered walls of the interior of the CHM's sapphire resonant cavity. This large wall relaxation rate is due to hydrogen interactions with paramagnetic impurities in the sapphire substrate that lies beneath the helium film.

- We measured the CHM's frequency stability relative to a room temperature hydrogen maser to be $\sigma_y(\tau) \approx 1.1 \times 10^{-13}/\tau^{1/2}$, for 10 sec $< \tau <$ 300 sec, where $\sigma_y(\tau)$ is the Allan deviation [8], a measure of fractional frequency stability over an averaging interval τ. Our measurements were limited by the stability of the room temperature hydrogen masers. For intervals longer than a few minutes, the CHM's frequency stability is not yet as good as that of a room temperature hydrogen maser. This long-term CHM frequency instability is a result of the large wall frequency shift due to the sapphire substrate lying beneath the superfluid helium film. A typical set of data comparing CHM and room temperature hydrogen maser frequency stability is shown in Figure 1, along with the calculated limit to CHM performance set by thermal noise.

- We improved the stability of the CHM's helium film thickness with the use of a quartz crystal microbalance (QCM) located between the film condensing impedance and the maser cavity. The QCM measures changes in the helium film thickness of less than 1% (less than 1 angstrom change) through the sensitive dependence of the QCM resonance frequency (~ 20 MHz) on mechanical loading by the helium film [9]. The resonance frequency of the QCM is compared to a stable reference oscillator, and

4

QCM frequency deviations are used as an indicator of helium film thickness variations. The resultant "error signal" is fed to a PID controller whose output adjusts the temperature of the condensing impedance to stabilize the helium film thickness at the QCM, and hence the maser.
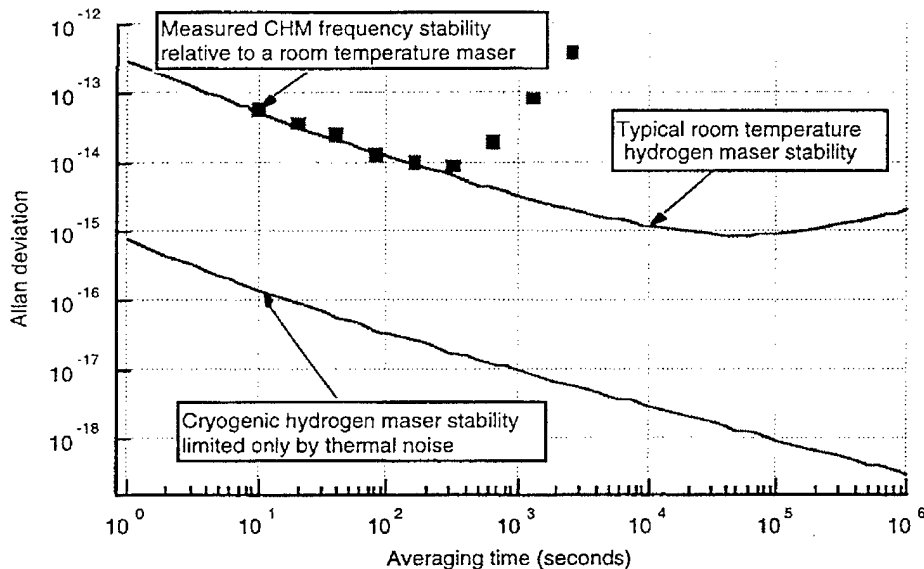

Fig. 1. Typical measured CHM and room temperature hydrogen maser frequency stabilities.

- We installed a thin-walled quartz bulb inside the sapphire resonant cavity to serve as the atomic hydrogen storage chamber. Quartz bulbs, coated on their interior with Teflon, are used successfully in this capacity in room temperature hydrogen masers built in our laboratory. This new quartz storage chamber will eliminate the large wall frequency shift observed in the CHM and allow excellent long-term CHM frequency stability to be achieved.

DBRM RESULTS

We recently developed a first-generation double-bulb rubidium maser (DBRM), shown in Figure 2. In this laboratory DBRM the resonant cavity at 6.835 GHz (the [87]Rb hyperfine frequency) is constructed of copper for low cost, ease of construction, and high Q. Magnetic shields, solenoids, and associated electronics were borrowed from our room temperature hydrogen masers (and hence are much larger than necessary). A heated-air system provides two regions of temperature control of ~ 0.1: one region for the maser bulb and resonant cavity, and one region for the pump bulb and rubidium reservoir. The sealed double-bulb cell is made of thin quartz with a tetracontane

5

($C_{40}H_{82}$) coating on its inner surface. The tetracontane coating was initially applied with a crude "melt-coat" technique: a macroscopic quantity of tetracontane was melted onto the quartz surface of the open double-bulb cell in air (i.e. before evacuation, rubidium transfer, and sealing). Two cavity-stabilized diode lasers optically pump ^{87}Rb into the desired $|F=2, m_F=0\rangle$ state. Using a 1.42 GHz signal acquisition system borrowed from our hydrogen masers, along with appropriate mixers and multipliers, we applied 6.835 GHz pulses to the state-selected ^{87}Rb atoms and detected hyperfine free-induction-decay signals (see Figure 3). We have not yet achieved active rubidium maser oscillation with the first-generation DBRM, because the ^{87}Rb depolarization rate with the crude melt-coat tetracontane surface is ~ 10 times greater than the depolarization rate measured by other investigators using a vapor-deposited tetracontane surface applied in vacuum [10,11]. We are working now to replicate these better wall coatings (see discussion below).
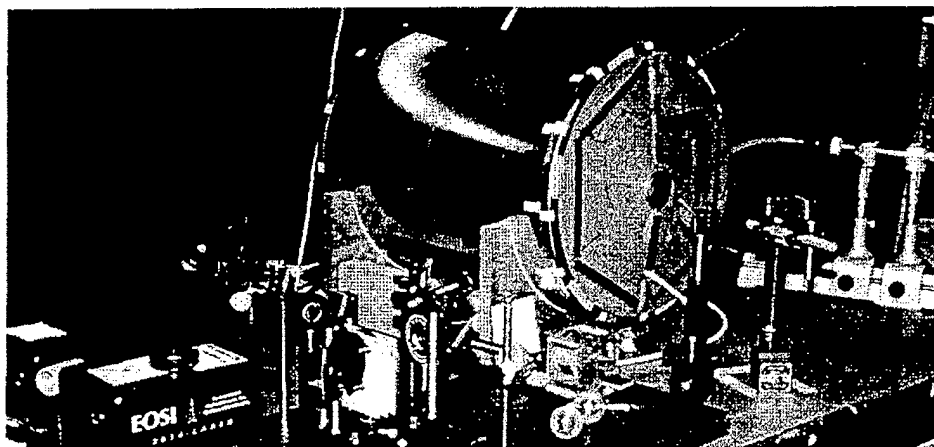

Fig. 2. Photograph of the first-generation double-bulb rubidium maser.

To create a DBRM tetracontane wall coating with a low depolarization rate, we are now using the vapor-deposition technique. To begin the coating process, we melt tetracontane onto a thin filament. We seal the filament inside the rubidium cell using standard glass-blowing techniques, and then evacuate the cell (to ~ 10^{-6} torr). We wrap a high Q rf coil outside the cell, which is inductively coupled to the filament within. We drive the coil with several watts of rf power; this rf energy is inductively coupled to the filament; and the filament and tetracontane heat. As a result the tetracontane evaporates from the filament and sticks on the walls of the cell, which are still at room temperature. This evaporative process deposits a thin but macroscopic layer of tetracontane on the cell walls. After several minutes of heating the filament, we stop the vapor coating process. Using glass-blowing

techniques, we remove the filament from the cell–while still under vacuum–
and chase rubidium into the cell.

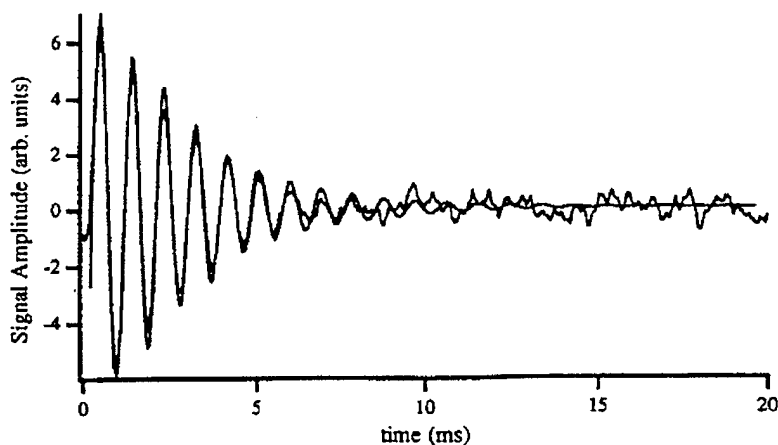
Fig. 3. Observed [87]Rb hyperfine free-induction-decay from the first-generation
DBRM.

We recently created several single-bulb rubidium cells with vapor-
deposited tetracontane wall coatings, and measured a low [87]Rb depolarization
rate consistent with past work [10,11] and sufficient to allow active DBRM
maser oscillation in a double-bulb quartz cell. The [87]Rb depolarization rate in
a cell may be measured using a well-known optical technique [12]. Two laser
beams, one strong and one weak, are focused on the same section of the cell.
The stronger laser beam is tuned spectrally and polarized appropriately to
optically pump the [87]Rb atoms in its path: for example this "pump beam"
may put all the [87]Rb atoms into one of the two hyperfine levels in the ground
electronic state (a hyperfine polarization), or it may create a Zeeman
polarization in either or both of the two hyperfine levels. The weaker "probe
beam" is configured to be at the same frequency and have the same
polarization as the pump beam, but not to be strong enough to noticeably
affect the [87]Rb polarization in the cell. (In our measurements we created the
probe beam by splitting off a small amount of the pump beam light.) The
probe beam will be absorbed by any unpolarized [87]Rb atoms in its path. Thus
we initially turn on the pump beam for several milliseconds to polarize the
sample; then we turn off the pump beam (using an optical chopper) and
monitor the transmission of the probe beam through the cell. With the
pump beam off, the [87]Rb atoms will begin to lose their polarization due to
wall collisions, Rb-Rb collisions, etc. As the polarization is lost, more of the
probe beam will be absorbed, and a weaker signal will be measured at a
photodetector. By measuring the decay in the intensity of the probe beam

7

propagating through the cell, we determine the ^{87}Rb depolarization rate for a particular cell. In several Pyrex test cells we have observed ^{87}Rb depolarization time constants ($\equiv T_1$ = inverse of depolarization rate) of ~ 30 milliseconds for wall temperatures and Rb densities similar to those planned for the DBRM. No difference in T_1 was observed between hyperfine and Zeeman polarization of the ^{87}Rb atoms. This measurement implies that ^{87}Rb atom state selection is completely lost after ~ 300 collisions with vapor-deposited tetracontane coated walls.

---

[1] J. Vanier and C. Audoin, *The quantum physics of atomic frequency standards* (Adam Hilger, Bristol, 1989).

[2] R.F.C. Vessot, et al., Phys. Rev. Lett. **45**, 2081 (1980).

[3] R.L. Walsworth, I.F. Silvera, E.M. Mattison, and R.F.C. Vessot, Phys. Rev. A **46**, 2495 (1992).

[4] M.E. Hayden, M.D. Hurlimann, and W.N. Hardy, Phys. Rev. A **53**, 1589 (1996).

[5] R.L. Walsworth, I.F. Silvera, H.P. Godfried, C.C. Agosta, R.F.C. Vessot, and E.M. Mattison, Phys. Rev. A **34**, 2550 (1986).

[6] A. Clairon, S. Ghezali, G. Santarelli, S.N. Lea, M. Bahoura, E. Simon, S. Weyers, and K. Szymaniec, Symposium on Frequency Standards and Metrology, edited by J. Bergquist (World Scientific, Singapore, 1996), 49.

[7] R.L. Tjoelker, J.D. Prestage, and L. Maleki, Symposium on Frequency Standards and Metrology, edited by J. Bergquist (World Scientific, Singapore, 1996), 33.

[8] D. Allan, Proc. IEEE **54**, 105 (1966).

[9] M.J. Lea, P. Fozooni, and P.W. Retz, *J. Low Temp. Phys.* **54**, 303 (1984).

[10] H.G. Robinson and C.E. Johnson, Appl. Phys. Lett. **40** (9), 771 (1982).

[11] C. Rahman and H.G. Robinson, IEEE J. Quant. Elect. **QE-23** (4), 452 (1987).

[12] A. Corney, *Atomic and Laser Spectroscopy* (Oxford University Press, Oxford, 1988), see chapter 17.